

PAPER

Classification of Gait Anomaly due to Lesion Using Full-Body Gait Motions

Tsuyoshi HIGASHIGUCHI[†], Toma SHIMOYAMA[†], *Nonmembers*, Norimichi UKITA^{†**a)}, *Senior Member*, Masayuki KANBARA[†], *Member*, and Norihiro HAGITA[†], *Fellow*

SUMMARY This paper proposes a method for evaluating a physical gait motion based on a 3D human skeleton measured by a depth sensor. While similar methods measure and evaluate the motion of only a part of interest (e.g., knee), the proposed method comprehensively evaluates the motion of the full body. The gait motions with a variety of physical disabilities due to lesioned body parts are recorded and modeled in advance for gait anomaly detection. This detection is achieved by finding lesioned parts a set of pose features extracted from gait sequences. In experiments, the proposed features extracted from the full body allowed us to identify where a subject was injured with 83.1% accuracy by using the model optimized for the individual. The superiority of the full-body features was validated in contrast to local features extracted from only a body part of interest (77.1% by lower-body features and 65% by upper-body features). Furthermore, the effectiveness of the proposed full-body features was also validated with single universal model used for all subjects; 55.2%, 44.7%, and 35.5% by the full-body, lower-body, and upper-body features, respectively.

key words: gait motion, full-body motion, lesioned part, 3D human skeleton

1. Introduction

The number of people suffering from chronic diseases is constantly rising. Today, more than three quarters of the elderly population are suffering from chronic diseases, independent of the economic, social, and cultural background [1]. Such diseases can be possibly avoided or decreased if people often undergo a medical examination and find the early symptoms of these diseases [2]. It is, however, difficult for most people to frequently have supports by experts such as medical doctors and therapists. In this work, we focus on the physical fitness of a lower body, in particular, a gait motion, which is crucial to maintain the quality of life.

As people get older, most of them may have the symptoms of lesions and/or aging on the lower body more or less. Such symptoms transfer in various ways such as insensitive sensation, and motor malfunction [3], [4]. These symptoms cause a change in the patterns of a gait motion [5]. Typical effects with aging in walking are characterized by various factors such as walking speed, step width, and leaning for-

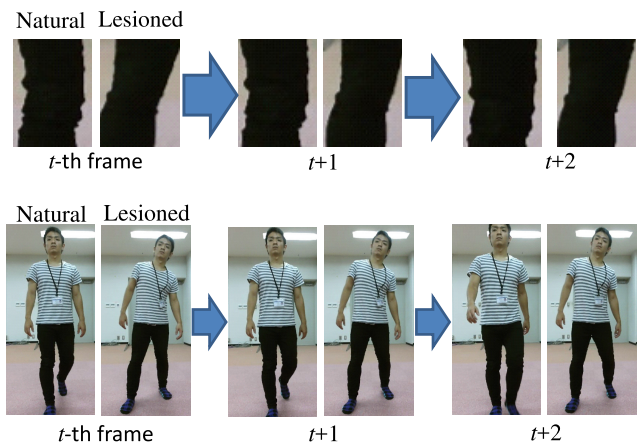


Fig. 1 Lesioned-part identification using a local appearance (upper row) versus a full-body appearance (lower row). In examples shown in this figure, the right knee of a subject was tightly bandaged. At each frame, gait-phase-synchronized bodies in a natural motion (left side at each frame) and a motion with a lesioned right knee (right side at each frame) are shown. While differences between these two motions at each frame are not significant, the pose of the full body with the lesioned right knee differs from the one in the natural motion.

ward angle [6]–[8]. The risk of falling is also affected by several stability factors (e.g., walking speed, toe clearance, and lateral body sway) [9]–[11].

This paper proposes a method for easy-to-use diagnosis that supports the evaluation of physical patterns in gait. For this evaluation, the proposed method classifies several symptoms of lesions on the lower body (e.g., knees and ankles), which are observed in gait.

For precisely evaluating symptoms observed in gait motions, our contribution is to employ appearance information extracted from the full body rather than local body parts such as knees and ankles. Figure 1 allows us to intuitively understand the effectiveness of the full body appearance. In the upper row, the local appearance of a lesioned right knee is shown. This local appearance reveals less difference between a natural motion (shown in the left-hand side at each frame) and a motion with a lesioned right knee (shown in the right-hand side at each frame). On the other hand, we can easily see differences between these two motions in the appearance of the full body shown in the lower row; for example, the upper body with the lesioned right knee is inclined backward and to the left for balancing. In this paper, a set of gait features is employed and appropriately pruned

Manuscript received August 9, 2016.

Manuscript revised December 1, 2016.

Manuscript publicized January 10, 2017.

[†]The authors are with Graduate School of Information Science, Nara Institute of Science and Technology, Ikoma-shi, 630-0192 Japan.

^{*}Presently, with Toyota Technological Institute.

^{a)} E-mail: ukita@toyota-ti.ac.jp

DOI: 10.1587/transinf.2016EDP7332

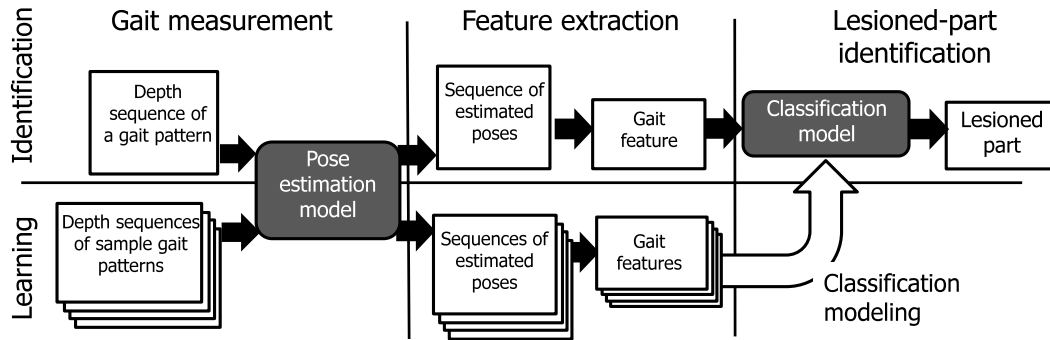


Fig. 2 Overview of the proposed method. The learning and identification steps are shown in lower and upper rows, respectively. Data are enclosed by rectangles and their flows are visualized by arrows in the figure.

for robust lesioned-part identification.

In contrast to our earlier work [12], additional experiments using the natural gait sequences of elderly people are also shown. Since all experiments in the earlier work used imitated gait data in which the lower-body of subjects were bandaged or immobilized, the additional experiments using the natural gait sequences are useful for verifying the effectiveness of the proposed method in real scenarios.

2. Related Work

The proposed method employs a depth sensor for the evaluation of a 3D gait motion, which is expected to be more informative for lesioned-part identification than silhouette-based gait motions [13]. The depth sensor is able to robustly reconstruct the 3D pose (i.e., 3D positions of joints) of a person of interest [14], [15] rather than a conventional RGB camera. A Kinect V2 sensor was used in our experiments, and its accuracy is better than that of Kinect V1 [16], [17] for several tasks related to gait analysis [18], [19].

While such a camera-based sensor can observe people only within its field of view, people are not required to carry any wearable sensors [20] and their motions are not affected by these sensors. In addition, for our goal (i.e., finding the symptoms in a gait motion), 24-hour observation using wearable sensors is not necessarily required.

A temporal sequence of a 3D body pose is defined as a gait motion. From the gait motion, we can extract several features representing physical symptoms caused by aging and/or physical disability. For these features, walking speed, stride, pace, etc. are useful [21]. For example, walking speed, stride, and pace become slow, short, and slow, respectively, due to the motor function decline [22]. As well as the walking speed, its acceleration is different between healthy people and elderly and/or disabled people [23], [24]. It is also known that the anteversion of pelvis becomes smaller and left-right asymmetric due to the hemiplegia arthrosis [25].

The aforementioned features are well known in the literature in physiotherapy and biomechanics. However, these features are extracted from only target body parts/joints in

previous work mentioned above. However, we know intuitively that not only the motion of lesioned part(s) but also the one of the full body is affected as the symptom of aging and/or physical disability. This paper proposes a method that identifies lesioned part(s) based on gait motion features extracted from the full body. While the closest work to our method is presented in [26], this method [26] analyzes the motion variation of the full body under an assumption that a lesioned body part is known. For the purpose of finding such lesioned part(s), this is a kind of chicken-and-egg problem. On the other hand, our proposed method finds lesioned part(s) and estimated their symptoms (i.e., how severe the symptom is) from gait features extracted from a temporal sequence of a 3D body pose.

3. Lesioned-Part Identification

3.1 Overview

The overview of the proposed method is illustrated in Fig. 2.

In its learning step (bottom row in Fig. 2), a number of gait patterns including the symptoms of lesions on various body parts are observed by a depth sensor, Kinect V2. Each observed depth sequence is used to estimate the sequence of 3D body poses (i.e., skeletons) by using a pose estimation model [14], [15], as shown in “Gait measurement” in Fig. 2. From the sequence of estimated 3D skeletons, a set of gait features are extracted. Since each set of gait features is labeled with the lesioned body part, a classifier (“Classification model” in Fig. 2) can be trained.

When the depth sequence of a gait motion is observed for lesioned-part identification, its gait features are extracted as in the learning step. Then the set of the gait features is classified in order to identify the lesioned part.

3.2 Gait Features Representing the Motion of the Full Body

A set of gait features are detected from the 3D skeletons of one gait cycle. This gait cycle is extracted from the observed sequence of the 3D skeleton so that each cycle begins and ends when the left knee is in front of and furthest from

the pelvis.

The 3D coordinates of the raw gait data are represented in Kinect's coordinate system with the origin set to the optical center of Kinect. The 3D coordinates of each gait data are spatially aligned so that (1) the z -axis coincides with the walking direction of a subject and the y -axis is equal to the vertical upward axis and (2) the origin at each frame coincides with the spine base. The walking direction is approximated by the 3D direction from the spine base at the beginning frame to that at the ending frame.

All gait cycles are temporally normalized so that all of them consist of the same number of frames. In the normalized gait cycle, the 3D skeleton of each frame (denoted by P_i for i -th frame) is synthesized from observed skeletons with linear interpolation:

$$P_i = \left(\frac{d_{i^{(+)}}}{d_{i^{(-)}} + d_{i^{(+)}}} \hat{P}_{i^{(-)}} \right) + \left(\frac{d_{i^{(-)}}}{d_{i^{(-)}} + d_{i^{(+)}}} \hat{P}_{i^{(+)}} \right)$$

where $\hat{P}_{i^{(-)}}$ and $\hat{P}_{i^{(+)}}$ denote the observed skeletons whose observed times are closest to the time of i -th frame. $\hat{P}_{i^{(-)}}$ and $\hat{P}_{i^{(+)}}$ are observed prior to and later than P_i , respectively. $d_{i^{(-)}}$ and $d_{i^{(+)}}$ denote respectively the time differences from the time of i -th frame to the observed times of $\hat{P}_{i^{(-)}}$ and $\hat{P}_{i^{(+)}}$.

From each frame in the normalized temporal sequence, the following gait features are computed:

1. Relative x, y, z positions between the mid-spine and each joint/endpoint
2. Relative x, y, z velocities between the mid-spine and each joint/endpoint
3. Relative x, y, z accelerations between the mid-spine and each joint/endpoint
4. Angle of each joint
5. Angular velocity of each joint
6. Walking velocity along a moving direction
7. x, y, z positions of a body centroid
8. x, y, z velocities of a body centroid

From a 3D skeleton reconstructed by a Kinect V2, relative positions, velocities, and accelerations from the mid-spine to the head, neck, pelvis, both shoulders, both elbows, both wrists, both groins, both knees, both ankles, and both feet (in total, 17 points) are computed for the aforementioned features 1, 2, and 3, respectively. Joint angles and angular velocities are computed in the spine, neck, both shoulder blades, both shoulders, both elbows, both groins, both knees, and both ankles (in total, 14 points) for the features 4 and 5, respectively. The joint angle (radian) of joint j is represented by the 3D position of j and those of j 's parent and child joints. A body centroid is determined based on a weight distribution in a human body; according to a report from a physiotherapy, the weights of the head, neck, both arms, torso, and both legs are 4%, 3%, 10%, 48%, and 35%, respectively.

In addition to eight features listed above, each of them is subtracted from the mean of natural gait motions in training data. These features are called mean-normalized features. In total, $8 + 8 = 16$ features are extracted from each

frame. All of these features extracted from all frames are concatenated to compose a gait feature vector.

3.3 Dimensionality Reduction of the Gait Feature

The dimension of the above mentioned gait feature vector is huge. Specifically speaking, the concatenation of 16 gait features is a 376-dimensional vector: $((17 \times 3) + (17 \times 3) + (17 \times 3) + 14 + 14 + 1 + 3 + 3) \times 2 = 376$. For improving the discriminativity of the gait feature vector, its dimension is reduced by two schemes, namely backward search (a.k.a. backward feature elimination) and linear discriminant analysis (LDA), as follows:

Step 1: Assume the current dimension of a gait feature is N . initially, $N = 376$. For backward search, all gait samples are divided into training and validation samples, and the training samples are used for producing $N + 1$ LDA modes below:

- A LDA model is trained with N components of all training samples.
- N LDA models are trained with $(N - 1)$ components of all training samples so that one of N components in the gait feature vector is not used for each of N LDA models.

Step 2: All of these $(N + 1)$ LDAs are tested with the validation samples.

Step 3: If one of LDA models with $(N - 1)$ components (which is trained without k -th component) gets the best score in this validation, this k -th component is removed from the gait feature vector. Then, go back to Step 1. Otherwise, namely if the LDA model with N components is the best, the backward search ends. This LDA model is used for lesioned-part identification.

With training data stored in the selected LDA model, k -Nearest Neighbor ($k = 3$ in our experiments) is employed for lesioned-part identification.

4. Experiments

4.1 Dataset Collection

For realistic applications, it's better to collect and use the data of people who are actually lesioned. It is, however, difficult to collect a number of such data. Instead of using only natural data, two kinds of gait data were collected. In the first one, spurious lesions were given to the body parts of subjects by bandaging or immobilizing them as shown in Fig. 3. The second one was the natural gait data of elderly people. Both kinds of gait data were observed in a laboratory setup (Fig. 4).

The spurious lesions, which were determined under the direction of a physiotherapist, emulate the functional decline of joints caused by aging; for example, bending and stretching the knee [27] and the plantar flexion and dorsiflexion of the ankle [28]. The following spurious lesions were given to

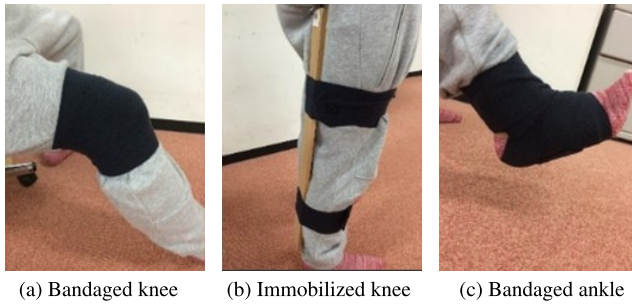


Fig. 3 Spurious lesions given for our experiments.



Fig. 4 Environment for capturing our gait dataset. A subject begins to walk in the acceleration area. While the subject walk through the measurement area, the temporal sequence of gait features are extracted.

physically-healthy people in our experiments:

Gait motion with bandaged knee(s): When the knee of a subject was bent 90 degrees, it was bandaged weakly or tightly. Each of both knees was bandaged. In addition to two by two combinations (i.e., left/right knees bandaged weakly/tightly), the gait motion of each subject was observed also when both knees were bandaged tightly. In total, five conditions were observed. The motion of a bandaged knee is similar to a decrease in the articular range of motion due to aging.

Gait motion with immobilized knee(s): When the knee of a subject was straight, it was immobilized with a splint. In this immobilization condition, the knee was almost immobilized. This condition is similar to the symptom of a muscle strain. Each of both knees was immobilized separately. That is, two conditions were observed for each subject.

Gait motion with bandaged ankle(s): When the ankle of a subject was bent 90 degrees, it was bandaged. For experiments, left ankle, right ankle, and both ankles were bandaged separately. In total, three conditions were observed for each subject.

As well as these 10 gait motions (i.e., 5 from bandaged knees, 2 from immobilized knees, and 3 from bandaged ankles), natural gait data with no bandage are measured. Eventually, 11 gait motions are defined for classification experiments.

Table 1 Effect of dimensionality reduction using backward search for lesioned-part identification. The mean of all gait motions is shown in each subject. For identification in i -th subject, training data of only i -th subject was used to train the LDA. For each subject, the best score is shown by **bold**.

Subjects	All features (%)	Selected features (%)
A	62.7	73.6
B	60.5	66.8
C	67.7	80.5
D	76.8	87.2
E	61.8	75.9
F	67.3	80.5
G	86.8	91.4
H	86.3	91.4
I	71.8	83.6
J	73.6	79.6
Mean	71.6	81.1

The spurious lesions were given to 10 subjects. All of them were twenties males. Each of 11 gait motions was captured 10 times for each subject. In total, 110 gait cycles were captured for each subject. Since only 10 twenties were measured, the variation of their gait patterns is limited.

The gait data of elderly people were captured in an elderly care house; Kyoto Yuyu-no-sato. Gait data were measured from 206 subjects ranging from 48 to 93 years old; the mean age was 78.5. While more subjects were also captured, their gaits were significantly different from others due to some severe physical disabilities. Since these disabilities were unknown unlike spurious lesions, these subjects were removed from the dataset used in this work. That is, only natural gait motions with no physical problems were observed from elderly people, and used for increasing the variation of gait data in order to bring our experiments closer to real scenarios.

4.2 Experiments Using Limited Variation of Gait Data: Model Optimized for the Individual

In Sects. 4.2 and 4.3, the proposed method is evaluated using only the gait dataset of 10 young subjects with spurious lesions. Since, in this dataset, the number of the subjects and the gait variation are small in contrast to those of the elderly-person dataset, lesioned-part identification is easier. After investigating the parameters of the proposed method with this easier dataset, the effectiveness of the proposed method is verified with a larger dataset in the next Sect. 4.4.

In this Sect. 4.2, all experiments were conducted so that the gait of i -th subject was tested with an individual model that was trained with only i -th subject's gait data. For each subject, a leave-one-out cross validation procedure was performed.

First of all, the effect of dimensionality reduction was investigated. In our experiments, feature selection using backward search was achieved by employing all data of all 10 subjects with the spurious legions. The result of this backward search was used for dimensionality reduction in all experiments shown in Sects. 4.2, 4.3, and 4.4. As the result of backward search, gait features (1), (5), (8), (1'),

Table 2 Confusion matrix of lesioned-part identification for 11 gait motions. All results were obtained with the selected features. The vertical and horizontal axes show the gait class of a query data and the estimated class, respectively. Values above 10 % are highlighted in gray cells.

Condition	Natural	Right knee			Left knee			Both knees	Right ankle	Left ankle	Both ankles
		Weak	Tight	Immobilized	Weak	Tight	Immobilized				
Natural	91.5	1.5	0.5	0	3.0	0.5	0	1.0	1.5	0.0	0.5
Right knee	Weak	0	84.0	12.0	0	1.5	0	0	1.5	1.0	0
	Tight	2.0	16.0	74.5	0	2.5	1.5	0	2.0	1.0	0
	Immobilized	0	1.0	1.5	95.5	0	0	0.5	1.5	0	0
Left knee	Weak	3.0	1.5	1.0	0	69.0	18.0	0	3.0	1.0	3.0
	Tight	2.0	0.5	2.5	0	24.0	57.5	0	4.5	1.0	6.5
	Immobilized	0	0	0	0	2.0	0	98.0	0	0	0
Both knees	0	2.5	3.5	0.5	1.5	2.5	0.5	88.0	0.5	0.5	0
Right ankle	0.5	1.0	3.0	0	2.5	1.0	0	1.5	81.5	1.0	8.0
Left ankle	1.5	0	0	0	6.0	3.5	0	0.5	4.0	74.5	10.0
Both ankles	0	0	1.0	0	2.0	0.5	1.0	0	8.5	9.5	77.5

Table 3 Confusion matrix of lesioned-part identification for 9 gait motions. Both for right and left knees, tightly- and weakly- bandaged motions were merged. All results were obtained with the selected features.

Condition	Natural	Right knee	Left knee	Both knees	Right ankle	Left ankle	Both ankles
Natural	90.0	5.0	2.0	1.0	0.5	1.0	0.5
Right knee	0.3	93.8	2.7	1.8	0.7	0	0.7
Left knee	1.3	2.7	91.7	1.3	0.7	2.0	0.3
Both knees	0	8.5	5.0	85.5	0.5	0.5	0
Right ankle	0.5	5.5	4.0	0.5	79.0	2.0	8.5
Left ankle	0.5	0	6.5	0	4.0	79.0	10.0
Both ankles	0	1.0	1.0	0.5	7.0	10.0	80.5

Table 4 3-class classification accuracy. This classification identifies the symptom on a lesioned part, after the initial classification, whose results are shown in Table 3, determines the lesioned part (right or left knees in examples shown in this table). The mean of classification accuracy is 77.1%.

	Right knee (%)	Left knee (%)
Weakly-bandaged	85.0	87.0
Tightly-bandaged	82.5	87.0
Immobilized	99.1	98.5

Table 5 Results of 3-class classification using local features. While this classification employs only several features extracted around a target part (i.e., right or left knee), the results shown in Table 4 were obtained with the features of the full body. The mean of classification accuracy is 65.0%.

Local features	Right knee (%)	Left knee (%)
Weakly-bandaged	58.0	69.5
Tightly-bandaged	44.0	50.0
Immobilized	85.5	83.0

(6'), (7'), and (8'), which are described in Sect. 3.2, were selected[†]. (*I'*) denotes the mean-normalized feature of feature (*I*). Comparison between results using all features and the selected features is shown in Table 1. This table shows the percentage of correctly-identified lesions. The performance was increased by around 10% on average.

With the selected features, a confusion matrix is computed. Each value in the confusion matrix is the mean of results for all subjects. Table 2 shows the results of lesioned-

part identification when all 11 kinds of gait motions were classified. The vertical and horizontal axes of the table show the gait class of a query data and the estimated class, respectively. This result is equivalent to the one shown in Table 1; the mean of diagonal values in Table 2 is 81.1, which is also shown as the mean in Table 1. As expected, it can be seen that it was difficult to discriminate between weakly- and tightly-bandaged knees.

To improve the discriminativity between different symptoms (e.g., weak and tight bandages) in the same body part, a two-step identification scheme was tested. In this scheme, only the position of lesion is identified initially. In our experiments, motions of tightly- and weakly- bandaged joints as well as immobilized joints were merged in each of right and left knees. If such a part is considered to be lesioned by the initial identification, the degree of the lesion is determined by a classification model that is trained by only the samples of lesions in this part; for example, the motions of weakly- and tightly-bandaged knees and immobilized knees are used for training for each of right and left knees. The results of initial classification (i.e., classification among 7 gait motions) are shown in Table 3. Table 4 shows the results of the second step where the motions of weakly- and tightly-bandaged knees and immobilized knees are classified after the initial classification. The final mean score of this two-step identification is 83.1%^{††}, which is 2% above

[†]For efficiency, backward search was executed so that (1) one gait feature is selected from 16 gait features and (2) all components in the selected gait feature were not used at each search step rather than each component of a gait feature vector.

^{††}This accuracy is computed from the diagonal values of the confusion matrix in Table 3 and the results of 3-class classification in Table 4 as follows: $(90.0 + 3 \times (93.8 \times \frac{85.0+82.5+99.1}{3}) + 3 \times (91.7 \times \frac{87.0+87.0+98.5}{3}) + 85.5 + 79.0 + 79.0 + 80.5) / 11 = 83.1$

Table 6 Confusion matrix of lesioned-part identification using gait features extracted from only the lower body.

Condition	Natural	Right knee			Left knee			Both knees	Right ankle	Left ankle	Both ankle
		Weak	Tight	Immobilized	Weak	Tight	Immobilized				
Natural	83.5	2.5	2.5	0	4.0	0.5	0	0.5	2.5	3.0	1.0
Right knee	Weak	0	64.5	27.0	0.5	2.0	0.5	0	4.0	0	0.5
	Tight	1.5	33.0	55.0	0.5	3.5	1.0	0	4.0	1.5	0
	Immobilized	0	1.5	2.0	95.0	0.5	0	0	0.5	0	0.5
Left knee	Weak	3.5	1.0	1.5	0	57.0	21.5	1.5	4.0	1.5	5.0
	Tight	1.0	1.5	0.5	0	33.5	55.0	0.5	3.5	1.0	2.5
	Immobilized	0	0	0	0	1.0	0.5	98.5	0	0	0
Both knees	1.0	2.5	2.5	0.5	4.5	3.5	1.0	83.5	0	0.5	0.5
Right ankle	2.5	1.5	3.0	0	2.0	0.5	0	0	78.5	2.0	10.0
Left ankle	1.5	0	1.0	0	4.5	2.0	0	0.5	4.5	74.0	12.0
Both ankles	0	0	0	0	3.0	1.5	0	0	11.5	14.0	70.0

Table 7 Confusion matrix of lesioned-part identification using gait features extracted from only the upper body.

Condition	Natural	Right knee			Left knee			Both knees	Right ankle	Left ankle	Both ankle
		Weak	Tight	Immobilized	Weak	Tight	Immobilized				
Natural	86.5	5.5	1.5	0.5	1.5	1.0	0	1.5	0.5	1.0	0.5
Right knee	Weak	3.5	68.5	14.5	1.0	4.5	0	0.5	3.0	3.0	0.5
	Tight	0.5	13.5	50.0	3.0	7.5	7.5	0.5	6.5	2.5	7.0
	Immobilized	1.0	2.0	4.5	85.5	0	1.0	0.5	2.5	2.0	0.5
Left knee	Weak	0.5	6.0	3.0	0	41.5	19.0	1.5	6.0	6.0	9.5
	Tight	2.5	2.0	4.0	0	23.0	43.0	1.0	6.5	2.0	6.0
	Immobilized	0	1.0	0.5	0.5	2.0	1.5	87.0	1.5	1.0	2.5
Both knees	1.5	3.5	10.5	1.0	5.5	6.5	1.5	61.0	4.0	3.5	1.5
Right ankle	0.5	2.5	4.0	0	7.0	4.0	0.5	3.0	53.0	12.5	13.0
Left ankle	0.5	1.5	2.5	0.5	8.5	6.0	0.5	1.0	12.0	53.5	13.5
Both ankles	0.5	2.5	2.0	0.5	8.0	4.0	0.5	2.5	7.5	15.5	56.5

Table 9 Mean percentage of correctly-identified lesions obtained by the two-step identification procedure. The best score in each column is shown by **bold**.

	Natural	Right knee			Left knee			Both knees	Right ankle	Left ankle	Both ankle	Mean
		Weak	Tight	Immobilized	Weak	Tight	Immobilized					
Full-body features	92	61	53	79	37	31	73	66	47	36	32	55.2
Lower-body features	89	38	29	80	21	25	77	48	32	27	26	44.7
Upper-body features	81	38	19	45	13	14	59	43	26	30	23	35.5

Table 8 Mean percentage of correctly-identified lesions obtained by the two-step identification procedure.

	Individual model (%)	Universal model (%)
Full-body features	81.1	66.0

the result shown in Tables 1 and 2.

Next, the effect of gait features extracted from the full body is validated. This effect is validated by comparing the results obtained using the full-body gait features with those using the features of a target body joint, which is called joint features. Results obtained using only joint features are shown in Table 5, where the target joints were right and left knees. Specifically, the joint features consist of gait features (1), (2), (3), (4), (5), (1'), (2'), (3'), (4'), and (5') where (l') denotes the mean-normalized feature of feature (l), all of which are described in Sect.3.2. Comparison between Tables 4 and 5 reveals the preponderance of the full-body features over the joint features.

For further analysis between full-body and joint fea-

tures, confusion matrices obtained using gait features of lower- and upper-body parts are shown in Tables 6 and 7, respectively. The joint features were used by the one-step identification procedure. The mean values of the percentages of correctly-identified lesions in Tables 6 and 7 are 74.1% and 62.4%, respectively, while the one computed by the one-step identification procedure using the full-body features is 81.1%. From these results, it has been demonstrated that the full-body features are useful for lesioned-part identification.

4.3 Experiments Using Limited Variation of Gait Data: Universal Model

In all experiments shown in Sect.4.2, a training data for each subject consists of only this subject's data; a classification model was trained individually. For the universal model that can be used for anybody, a classification model must be trained by training data of all subjects and applied

to anybody. To examine the effectiveness of the universal model, the percentage of correctly-identified lesions was computed with a leave-one-out cross validation procedure. The mean percentage among all subjects and all gait motions was shown in Table 8. The mean percentage of the universal model, 66%, is much lower than the one computed with individual models, 83.1%. This is a natural consequence because people have their own gait patterns, which are utilized for gait recognition [29].

4.4 Experiments Using Large-Scale Gait Data over a Wide-age Range: Universal Model

The dataset used in Sect. 4.2 was augmented with 206 natural gait motions of elderly people. The universal model was evaluated again for 10 twenties with a leave-one-out cross validation procedure, but all the models were trained also with all the 206 natural gait motions of elderly people. This was the difference from the experiments shown in Sect. 4.3.

Table 9 shows that the full-body features outperformed other two local features obtained from upper- and lower-bodies. While classification using the full-body features is superior to the local features in the universal model also, the performance of the universal model is much lower than that of the individual models; 55.2% vs 83.1%. For practical use, this classification performance should be insufficient. Since the effectiveness of the individual model has been demonstrated in this paper, a prospective solution is that the model optimized for the individual is produced by domain adaptation [30] from a small amount of data of each user and the universal model trained by a large number of people.

5. Concluding Remarks

This paper proposed a method using a depth sensor for finding the symptoms of lesions on the lower body. For finding the lesioned part and its degree of lesion, the proposed method employs a set of gait features representing the motion of the full body rather than local features around each body part. Compared with the local features, the effectiveness of the full-body gait features was demonstrated in experiments; for example, 74.1% by the lower-body features vs 83.1% by the full-body features using the two-step identification in the individual models, and 44.7% by the lower-body vs 55.2% by the full-body in the universal models.

Future work includes improvement of universal models for more general use. In addition, measurement noise may disturb correct lesioned-part identification. For example, it is reported that RMSEs for knee and hip joints in a gait sequence are 28.5 degrees and 11.8 degrees, respectively, in [18]. More comprehensive error analysis was conducted in [16]. By reducing such error by employing a human motion prior for pose tracking [31]–[33], it is expected that the identification performance of the proposed method is improved. Experiments using gait data with real lesions are also important for verifying the proposed method in more realistic scenarios. To this end, the gait data of elderly people whose

motion was significantly different from others might be used so that such data can be annotated manually by physiotherapists or specialists for gait diagnosis/rehabilitation.

This study was supported by Yanmar Lab 2112 and JSPS KAKENHI Grant Number 15H01583.

References

- [1] D.J. Vergados, A. Alevizos, A. Mariolis, and M. Caragiozidis, "Intelligent services for assisting independent living of elderly people at home," *PETRA*, p.79, 2008.
- [2] E.L. Cadore, L. Rodríguez-Mañas, A. Sinclair, and M. Izquierdo, "Effects of different exercise interventions on risk of falls, gait ability, and balance in physically frail older adults: a systematic review," *Rejuvenation Res.*, vol.16, no.2, pp.105–114, 2013.
- [3] M. Kaneko and M.P. Stryker, "Sensory experience during locomotion promotes recovery of function in adult visual cortex," *eLife*, vol.3, no.3, 2014.
- [4] B. Weinberger, D. Herndler-Brandstetter, A. Schwanninger, D. Weiskopf, and B. Grubeck-Loebenstein, "Biology of immune responses to vaccines in elderly persons," *Clin Infect Dis.*, vol.46, no.7, pp.1078–1084, 2013.
- [5] L.D. Duffell, D.F.L. Southgate, V. Gulati, and A.H. McGregor, "Balance and gait adaptations in patients with early knee osteoarthritis," *Gait & posture*, vol.39, no.4, pp.1057–1061, 2014.
- [6] H.B. Menz, S.R. Lord, and R.C. Fitzpatrick, "Age-related differences in walking stability," *Age and Aging*, vol.32, no.2, pp.137–142, 2003.
- [7] M. Schimpl, C. Moore, C. Lederer, A. Neuhaus, J. Sambrook, J. Danesh, W. Ouweland, M. Daumer, and A. Lucia, "Association between walking speed and age in healthy, free-living individuals using mobile accelerometry — a cross-sectional study," *PLoS ONE*, vol.6, no.8, p.e23299, 2011.
- [8] M. Lövdén, S. Schaefer, A.E. Pohlmeier, and U. Lindenberger, "Walking variability and working-memory load in aging: A dual-process account relating cognitive control to motor control performance," *The journals of gerontology. Series B, Psychological sciences and social sciences*, vol.63, no.3, pp.121–128, 2008.
- [9] J.M. Hausdorff, M.E. Nelson, D. Kaliton, J.E. Layne, M.J. Bernstein, A. Nuernberger, and M.A.F. Singh, "Etiology and modification of gait instability in older adults: a randomized controlled trial of exercise," *J. Appl. Phys.*, vol.90, no.6, pp.2117–2129, 2001.
- [10] B. Mariani, S. Rochat, C.J. Büla, and K. Aminian, "Heel and toe clearance estimation for gait analysis using wireless inertial sensors," *IEEE Trans. Biomed. Eng.*, vol.59, no.11, pp.3162–3168, 2012.
- [11] D.D. Espy, F. Yang, T. Bhatt, and Y.C. Pai, "Independent influence of gait speed and step length on stability and fall risk," *Gait Posture*, vol.32, no.3, pp.378–382, 2010.
- [12] T. Higashiguchi, T. Shimoyama, N. Ukita, M. Kanbara, and N. Hagita, "Lesioned-part identification by classifying entire-body gait motions," *PSIVT*, pp.136–147, 2015.
- [13] C. Zhou, I. Mitsugami, and Y. Yagi, "An attempt to detect impairment by silhouette-based gait feature," Annual Meeting of the European Society for Movement Analysis in Adults and Children, Glasgow, Scotland, Sept. 2013.
- [14] J. Shotton, A.W. Fitzgibbon, M. Cook, T. Sharp, M. Finocchio, R. Moore, A. Kipman, and A. Blake, "Real-time human pose recognition in parts from single depth images," *CVPR*, pp.1297–1304, 2011.
- [15] R.B. Girshick, J. Shotton, P. Kohli, A. Criminisi, and A.W. Fitzgibbon, "Efficient regression of general-activity human poses from depth images," *ICCV*, pp.415–422, 2011.
- [16] Q. Wang, G. Kurillo, F. Ofli, and R. Bajcsy, "Evaluation of pose tracking accuracy in the first and second generations of microsoft kinect," International Conference on Healthcare Informatics,

- pp.380–389, 2015.
- [17] S. Zennaro, M. Munaro, S. Milani, P. Zanuttigh, A. Bernardi, S. Ghidoni, and E. Menegatti, “Performance evaluation of the 1st and 2nd generation kinect for multimedia applications,” *International Conference on Multimedia and Expo*, 2015.
- [18] X. Xu, R.W. McGorry, L.-S. Chou, J.-H. Lin, and C.-C. Chang, “Accuracy of the microsoft kinect for measuring gait parameters during treadmill walking,” *Gait & Posture*, vol.42, no.2, pp.145–151, 2015.
- [19] B. Galna, G. Barry, D. Jackson, D. Mhiripiri, P. Olivier, and L. Rochester, “Accuracy of the microsoft kinect sensor for measuring movement in people with parkinson’s disease,” *Gait & Posture*, vol.39, no.4, pp.1062–1068, 2014.
- [20] P.E. Taylor, G.J.M. Almeida, T. Kanade, and J.K. Hodgins, “Classifying human motion quality for knee osteoarthritis using accelerometers,” *Annual International Conference of the IEEE Engineering in Medicine and Biology Society*, pp.339–343, 2010.
- [21] A.M. de-la Herran, B. Garcia-Zapirain, and A. Méndez-Zorrilla, “Gait analysis methods: An overview of wearable and non-wearable systems, highlighting clinical applications,” *Sensors*, vol.14, no.2, pp.3362–3394, 2014.
- [22] M. Brooke Salzman, “Gait and balance disorders in older adults,” *Am Fam Physician*, vol.82, no.1, pp.61–68, 2010.
- [23] M.O. Derawi, P. Bours, and K. Holien, “Improved cycle detection for accelerometer based gait authentication,” *Sixth International Conference on Intelligent Information Hiding and Multimedia Signal Processing*, pp.312–317, 2010.
- [24] W. Tao, T. Liu, R. Zheng, and H. Feng, “Gait analysis using wearable sensors,” *Sensors*, vol.12, pp.2255–2283, 2012.
- [25] M. Manca, G. Ferraresi, M. Cosma, L. Cavazzuti, M. Morelli, and M.G. Benedetti, “Gait patterns in hemiplegic patients with equinus foot deformity,” *BioMed Research International*, vol.2014, pp.1–7, 2014.
- [26] T. Ogawa, H. Yamazoe, I. Mitsugami, and Y. Yagi, “The effect of the knee braces on gait — toward leg disorder estimation from images,” *Proc. 2nd Joint World Congress of ISPGR and Gait and Mental Function*, Akita, Japan, Jun. 2013.
- [27] H. Sugiura and S. Demura, “The effects of knee joint pain and disorders on knee extension strength and walking ability in the female elderly,” *Advances in Physical Education*, vol.2, no.4, pp.139–143, 2012.
- [28] E. Simoneau, A. Martin, and J.V. Hoecke, “Muscular performances at the ankle joint in young and elderly men,” *J Gerontol A Biol Sci Med Sci.*, vol.60, no.4, pp.439–447, 2005.
- [29] J. Wang, M.F. She, S. Nahavandi, and A.Z. Kouzani, “A review of vision-based gait recognition methods for human identification,” *DICTA*, pp.320–327, 2010.
- [30] E. Tzeng, J. Hoffman, T. Darrell, and K. Saenko, “Simultaneous deep transfer across domains and tasks,” *ICCV*, pp.4068–4076, 2015.
- [31] N. Ukita, M. Hirai, and M. Kidode, “Complex volume and pose tracking with probabilistic dynamical models and visual hull constraints,” *ICCV*, pp.1405–1412, 2009.
- [32] N. Ukita and T. Kanade, “Gaussian process motion graph models for smooth transitions among multiple actions,” *Computer Vision and Image Understanding*, vol.116, no.4, pp.500–509, 2012.
- [33] N. Ukita, “Simultaneous particle tracking in multi-action motion models with synthesized paths,” *Image Vision Comput.*, vol.31, no.6-7, pp.448–459, 2013.



Tsuyoshi Higashiguchi got the M.E. degree from Nara Institute of Science and Technology. His research theme was evaluation of human physical motion such as gait.



Toma Shimoyama got the M.E. degree from Nara Institute of Science and Technology. His research theme was human motion diagnosis such as anomaly detection in gait.



Norimichi Ukita is a professor at the graduate school of engineering, Toyota Technological Institute (TTI), Japan. He received the Ph.D. degree in Informatics from Kyoto University, Japan, in 2001. After working for five years as an assistant professor at NAIST, he became an associate professor in 2007 and moved to TTI in 2016. He was a research scientist of PRESTO, JST from 2002 to 2006, and a visiting research scientist at Carnegie Mellon University from 2007 to 2009. His main research interests are multi-object tracking and human pose and activity estimation.



Masayuki Kanbara received a Ph.D. degree in engineering from Nara Institute of Science and Technology (NAIST) in 2002. He was an assistant professor at the Information Science Department at NAIST since 2002. He was a visiting researcher of University of California, Santa Barbara in 2008-2009. He has been an associate professor at NAIST since 2010. Fields of research are focused on augmented reality, computer vision and Human-Robot Interaction.



Norihiro Hagita received the Ph.D. degree in electrical engineering from Keio University in 1986. In 1978, he joined Nippon Telegraph and Telephone Public Corporation (Now NTT). He is currently Board Director of ATR and ATR Fellow, director of the Social Media Research Laboratory Group and the Intelligent Robotics and Communication Laboratories. He is the chairman of ATR Creative. He is also a visiting professor of Nara Institute of Science and Technology, Osaka University, and Kobe University. His major interests are cloud networked robotics, human-robot interaction, ambient intelligence, pattern recognition and learning, and data-mining technology. He has served as a chairman of technical committee in Network Robot Forum in Japan.